

# Construction of the $\mu$ RWELL Detector

Undergraduate Research Report by Sarah Arends  
Research Advisor: Dr. Marcus Hohlmann

**Abstract**—During the Fall 2018 semester, a 10cm by 10cm micro-resistive well detector was investigated and constructed by undergraduate researchers in the High Energy Physics (HEP) Research group at Florida Tech. The detector will undergo a series of quality controls to assess its performance.

## I. BACKGROUND AND DETECTOR DESIGN

The micro-resistive well ( $\mu$ RWELL) detector is classified as a micro-pattern gas detector (MPGD) with a single amplification stage. In this regard, the design differs from the gas electron multiplier (GEM) detectors that have previously been studied in this lab, as GEMs have a three-stage amplification process. The readout and amplification mechanisms of the  $\mu$ RWELL are built into the printed circuit board (PCB) of the detector, as shown in figure 1. A polyimide foil of 50 micron thickness contains an array of cone shaped holes that are responsible for the amplification of the signal charge [2]. The charge is then induced and spread on a resistive layer of Diamond-Like Carbon (DLC) that is separated from the readout electrode below by a layer of glue. A drift cathode is placed above the PCB, and the space between these two structures defines the drift gap. In the case of the 10cm by 10cm detector being studied this semester, the readout is also mounted on a honeycomb structure for additional support.

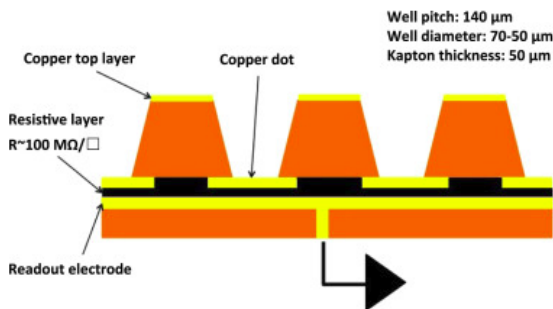


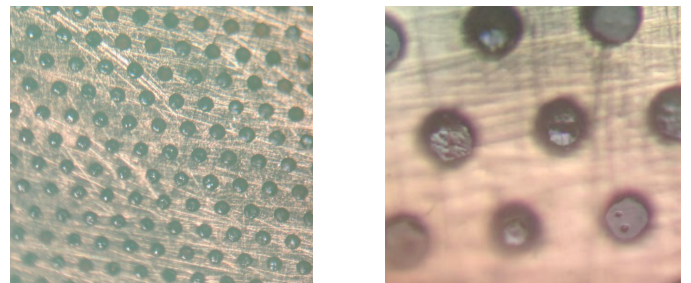
Fig. 1: A schematic of the PCB of the  $\mu$ RWELL detector

The microscopic scale of MPGDs typically leaves them susceptible to unwanted electrical discharge, in the form of sparking, which can hinder the performance of the detector or potentially damage electronic instrumentation [1]. The addition of the resistive layer at the base of the wells limits the amplitude of the discharge in order to prevent such an issue, and it also allows for high detector gain.

## II. INSPECTION OF THE FAULTY FOIL

Before the arrival of the full detector shipment intended for construction, a "problematic" foil was received for preliminary investigation. The wells on the  $\mu$ RWELL foil should have a

diameter of approximately 70 microns, but an issue in the manufacturing resulted in a larger diameter of the holes - approximately 80 microns. The thickness of this foil was measured to be  $0.18 \pm 0.0072$  millimeters. In order to test the viability of a cylindrical detector design, the foil was placed in a mount and bent in an inward and outward-facing orientation with a radius up to 1 inch. There did not appear to be any disfiguration, such as delamination, as a result of this bending. The curvature of the foil would pose a problem if it began to affect the gain of the detector, but unfortunately the foil could not be accessed in an appropriate manner to test this factor.



(a) The array of conical wells in the copper-coated polyimide foil

(b) Texture visible in the base of the wells under greater magnification

Fig. 2: Images taken under a microscope of the well structure

A microscope calibration slide was used to measure the diameter of the wells on the foil, and a value of  $81.2 \pm 1.7$  microns was obtained. Because the microscope had difficulty focusing on the wells and the calibration scale simultaneously, the measurements suffered from a source of random error. This error was minimized by performing a large sample of measurements.

The foil was probed with an MIT 420/2 Megger in order to examine connectivity among its components. The traces are insulated with a polyimide layer, with the exception of the pads intended for the panasonic connection and the last few millimeters of each strip on the end nearest the active region. This provides two points of contact for the traces.

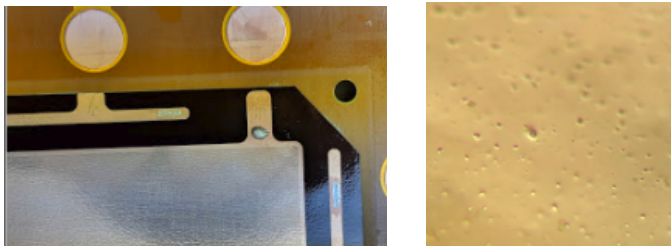
Background research was conducted to determine an expected value for the resistivity of the DLC. One report indicated a resistivity of  $12M\Omega$  per square for a 10cm x 10cm chamber with comparable well diameter. Voltage was applied between the copper layer above the polyimide foil and the signal traces, which were connected with a strip of copper tape in order to observe the contribution of the entire active region. For each voltage applied, the resistance reading exceeded the maximum rating of the Megger. This is a reasonable result, as one should only see current if there is a strong electric field

present in the wells. Otherwise, a short would be present in the foil.

We applied voltage to the copper top layer relative to the signal and ground traces. We saw high resistance/ no current, which makes sense. It should only be connected via a strong electric field. A connection in the current configuration would imply a short.

### III. INVESTIGATION OF THE DLC

The contents of the  $\mu$ RWELL detector kit were initially inspected upon arrival. Some tarnish was visible on the active region, which was then investigated under the microscope. In the process, a texture constituting small "bumps" was visible at the base of the wells. Note that this does not seem correlated to the tarnish on the surface. It was hypothesized that this texture was a consequence of the DLC, and an investigation was conducted to determine if this could be accessed from any location other than the base of the wells. As seen in figure 3a, a dark layer of material extends beyond the active region of the board and beneath the grounding ring. When viewed under the microscope, the material, shown in figure 3b, possesses the same bumpy texture seen in the base of the wells. If this was an exposed area of the DLC, one would be able to measure its resistivity. However, meggering across a small distance in this region yielded a resistance over the maximum rating of the Megger for applied voltages up to 200V. A visual scan of any inconsistencies or damage around this material was conducted to determine the nature of the layering. Ultimately, confirmation was received that the DLC is completely covered with polyimide, and therefore it is not accessible for measurements.



(a) Dark material extending beyond active region and grounding ring (b) Bubbles seen on this dark material

Fig. 3: Microscope images of the dark material on the PCB

Measurements were taken again with the microscope calibration slide in order to determine the upper and lower diameters of the wells (recall they have a conical form). However, it proved very difficult to distinguish clearly between the boundaries of the upper and lower holes, shown in table I. Nevertheless, measurements were taken for both quantities and yielded the following results.

### IV. CHAMBER PREPARATION AND CONSTRUCTION

Measurements of the outer frame and o-rings were taken to ensure there were no large disparities that would prevent gas tightness of the chamber. Readings obtained from the

TABLE I:  
Well Diameters

Upper Diameter	$31.3 \pm 1.8 \mu\text{m}$
Lower Diameter	$79.7 \pm 3.7 \mu\text{m}$

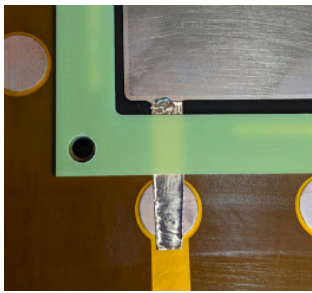
groove meter required an offset to be added to account for the protruding tip of the meter. The thickness of the o-ring was measured with a Vernier caliper.

TABLE II:  
Groove Depth and O-ring Measurements

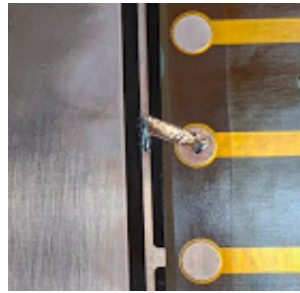
Top Groove Depth	$1.834 \pm 0.014 \text{ mm}$
Bottom Groove Depth	$1.866 \pm 0.024 \text{ mm}$
Top O-Ring Thickness	$2.904 \pm 0.020 \text{ mm}$
Bottom O-Ring Thickness	$2.903 \pm 0.023 \text{ mm}$

In order to apply voltage to the active region of the detector, an external point of access must be available. To create such a connection, a strip of copper tape was soldered between a protruding tab on the active region and a neighboring high voltage (HV) pad, as shown in figure 4a. This pad, which is located adjacent to the inner frame stack, is connected to another pad outside the outer frame via a connection within the PCB. In this way, no new connections are created than run underneath the outer frame, preventing gas tightness. Caution was also taken to prevent solder from sitting below the inner stack frames and disrupting its placement, as this could alter the uniformity of the drift gap. A similar soldered connection was established between an HV pad and the grounding ring that surrounds the active region. This can be seen in figure 4b. A low resistance was measured through these new connections to ensure good conductivity and prevent electrical issues later on. The grounding ring was connected to the ground of the board by soldering a wire from the HV pad to the copper perimeter on the board. This board ground is also electrically connected to some of the traces intended for the panasonic connector. Therefore, another ground connection will be established when the panasonic is installed. When charge is diffused across the active region, it can be collected at the grounding ring and flow out into the grounded connection. Without the presence of this ring, the active area may charge up and could distort the electric fields required for proper functioning.

The detector shipment arrive with plastic screws, required to hold the inner frame stack in place. The screws are inserted from the bottom of the detector, and held in place with a nut after building the inner stack (frames and drift foil). However, these screws were too long and thus prevented the detector from being closed properly. The screws were trimmed by approximately 0.56 mm with an X-Acto knife, and a file was used to clean up the cut afterwards. Before re-inserting into the detector, the screws were also cleaned in an ultrasonic bath and thoroughly dried. To maintain gas tightness around the point of insertion of the screws, the screw heads were coated with an Araldite adhesive.



(a) Active region soldered to adjacent hv pad, which will connect to a pad outside the sealed chamber



(b) Grounding ring connected to adjacent hv pad

Fig. 4: Soldered connections on detector PCB

For this initial assembly, a drift gap of 3mm was formed by 5 layers of 0.5 mm spacers. Note that the drift foil itself sits between 0.5mm spacers, which contributes 0.5mm to the drift gap. After installing the drift foil, a connection had to be created between the drift tab and an external pad, so that the drift can be accessed after closing. A copper strip was soldered between the drift tab and an adjacent hv pad, as shown in figure 5 in order to create the connection.

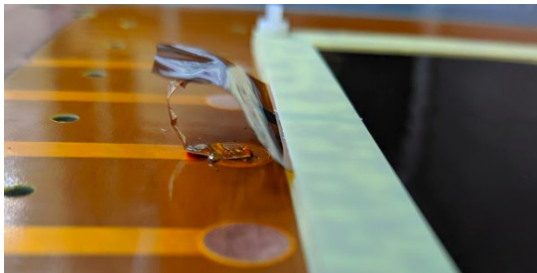


Fig. 5: Drift tab soldered to hv pad through copper strip

The outer frame required some additional preparation before closing the chamber. The frame was prepared for installation of the gas plugs by drilling two holes on opposite sides of the frame with a 3/32 drill bit and threading the holes with an M3 tap. The outer frame was cleaned in the ultrasonic bath, and a resin coating was applied to the interior of the frame. The gas plugs were installed in the outer frame and sealed with an Araldite adhesive.

After the stack and outer frame preparations were complete, the detector was completed by installing the polyimide window and lid and sealing with the closing screws. Caution was taken to clean all components of the detector, especially the active region, before closing the detector in order to prevent any particulate contamination that could cause sparking. The screws were initially installed by hand from the bottom of the chamber and held in place with accompanying nuts.

## V. QUALITY CONTROL TESTING

The  $\mu$ RWELL detector will undergo quality control tests similar to those conducted on GEM detectors during their quality assurance process. The QC3 test will ensure the detector is able to maintain sufficient internal pressure when

the chamber is pressurized to 5mbar. Gas tubing was created to adapt the existing system in the clean room for testing of the  $\mu$ RWELL. The system, shown in part by figure 6, was pressurized before connecting the detector in order to ensure the system and new tubing was functioning properly. After inserting the detector in the system, a preliminary test of QC3 was conducted but failed to pass. The screws were tightened again with a screwdriver, while the nuts were held in place with a wrench. This adjustment seemed to reduce the leak rate to some extent, but efforts are still ongoing to ensure the detector meets the standard for gas tightness.

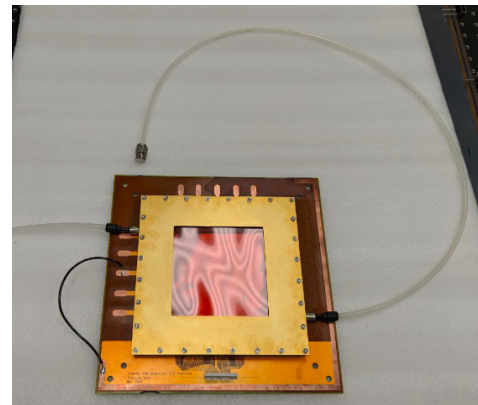


Fig. 6: The  $\mu$ RWELL detector assembled and attached to gas lines in preparation for the QC3 gas leakage test

Afterwards, the QC4 high voltage test will be conducted to ensure proper function of the HV circuit on the detector and quantify the amount of spurious signals. Once this test has passed, the QC5 test will quantify the gain of the detector and response uniformity.

## VI. PROJECT OUTLOOK

After quality control testing has successfully been completed on the  $\mu$ RWELL detector, a potential continuation of the study would include varying the drift gap. This would alter the preliminary ionization of the chamber, and the effect on the detector gain could be studied.

Incoming students are working alongside current researchers so that this project may continue even as some of its members leave. Research reports such as this one can serve as legacy documentation for future students who wish to gain insight into the developments made and challenges faced in the project's history.

## REFERENCES

- [1] G. Bencivenni et al, "Performance of mu-RWELL detector vs resistivity of the resistive stage," Nuclear Instruments and Methods in Physics Research Section a-Accelerators Spectrometers Detectors and Associated Equipment, vol. 886, pp. 36-39, 2018.
- [2] M. Poli Lener et al, "The -RWELL: A compact, spark protected, single amplification-stage MPGD," Nuclear Instruments and Methods in Physics Research, Section A: Accelerators, Spectrometers, Detectors and Associated Equipment, vol. 824, pp. 565-568, 2016.